

# A Soft Approach to Encapsulate Sulfur: Polyaniline Nanotubes for Lithium-Sulfur Batteries with Long Cycle Life

Lifen Xiao, Yuliang Cao,\* Jie Xiao, Birgit Schwenzer, Mark H. Engelhard, Laxmikant V. Saraf, Zimin Nie, Gregory J. Exarhos, and Jun Liu\*

Applications of rechargeable batteries are diverse and range from storing energy from renewable resources such as wind generators and solar arrays, powering electric vehicles and portable electronic devices. Significant R&D efforts have focused on achieving high energy density, long cycling life, low cost, and safety.<sup>[1]</sup> Among all known rechargeable battery systems, lithium-sulfur (Li-S) batteries have attracted considerable attention. Elemental sulfur is abundant, and is a very attractive cathode material for lithium batteries because of its high theoretical capacity (1672 mAh g<sup>-1</sup>) and specific energy (2600 Wh kg<sup>-1</sup>), assuming complete reaction of lithium with sulfur to form Li<sub>2</sub>S.<sup>[2]</sup>

Despite these advantages, practical applications of Li-S batteries are limited by several problems. One is the electrical insulating nature of elemental sulfur ( $5 \times 10^{-30}$  S cm<sup>-1</sup> at 25 °C) and the discharge products, which lower both the electrochemical activity and utilization of sulfur. This problem can be resolved effectively by dispersing sulfur into a conductive matrix (e.g., polymers and/or carbon networks).<sup>[3]</sup> Another issue associated with Li-S system is the poor cyclability, which results from the high solubility of the intermediate products, lithium polysulfides Li<sub>2</sub>S<sub>x</sub> ( $2 \leq x \leq 8$ ).<sup>[4]</sup> The polysulfides can diffuse to the lithium anode where they are reduced to short-chain polysulfides. Those soluble species also can move back to the cathode and be reoxidized into long-chain polysulfides. This parasitic process creates an internal shuttle reaction that results in low coulombic efficiency. Moreover, a fraction of the soluble polysulfides are strongly reduced to insoluble Li<sub>2</sub>S<sub>2</sub> and/or Li<sub>2</sub>S, which are then deposited on the anode surface and gradually form a thick layer during repeated cycling. The same phenomenon also occurs on the cathode surface during discharge. The

deactivated insoluble agglomerates on both electrodes can lead to a progressive loss of active materials, inaccessibility of the active components in the electrode, degradation of the electrode structure, and increased cell impedance. These cumulative effects then are reflected in the rapid capacity fading of Li-S battery upon charge/discharge cycling.

Extensive research has been conducted to address the challenges described above. One approach is to use alternative electrolytes and electrolyte additives to mitigate the solubility problem of the polysulfides in the electrolyte.<sup>[5]</sup> The other approach is to tailor the conductive matrix to support good conductivity and dispersion of sulfur and also constrain sulfur and the polysulfides within the framework. Many different porous carbon materials have been studied.<sup>[6]</sup> Nazar et al.<sup>[6a]</sup> used ordered mesoporous carbon to encapsulate the sulfur species within resident nanochannels. This composite, coated with an additional thin-layer polymer, showed a high initial reversible capacity of 1320 mAh g<sup>-1</sup> with promising cycling ability confirming the feasibility of their novel concept. Most recently, porous hollow carbon spheres with an interior void space and a mesoporous shell structure composed of sulfur exhibited a high initial reversible capacity of 1071 mAh g<sup>-1</sup> at a 0.5 C rate and maintained 91% capacity retention after 100 cycles.<sup>[6b]</sup> Furthermore, Cao et al. and several groups have also reported the use of graphene sheets to confine the sulfure compounds.<sup>[7]</sup> Although carbon-based materials are attractive, many synthesis procedures use a multistep, hard-template approach that requires removal of the template in a late stage. The different carbon structures greatly improved the stability of the electrode, but the capacity fading is still a problem. Recently, Ji et al.<sup>[8]</sup> borrowed a concept from drug release and incorporated mesoporous silica into the carbon matrix. The mesopores function as a reservoir for the deposition and subsequent reversible desorption and release of the sulfide products.

Polymer materials have been widely used for drug delivery and are effective in encapsulating and controlling the release of desired chemicals in the internal pore space within the polymer matrix. Indeed, conductive polymers, such as polythiophene and polypyrrole containing different tailored porosities, have been explored as matrices to physically absorb and hold sulfur.<sup>[9]</sup> Wu et al.<sup>[9b]</sup> constructed a sulfur/polythiophene composite with a core/shell structure. The composite produced a high initial discharge capacity of 1119 mA g<sup>-1</sup> and retained 69.5% of the capacity after 80 cycles. These results show that a simple physical confinement and absorption process is not sufficient in retarding polysulfide dissolution to provide an adequate cycle life while still retaining high capacity. Several groups have explored polyacrylonitrile (PAN)/S systems.<sup>[10]</sup> It

Dr. L. Xiao, Dr. Y. Cao, Dr. J. Xiao, Dr. B. Schwenzer, Dr. M. Engelhard,  
Dr. L. Saraf, Dr. Z. Nie, Dr. G. Exarhos, Dr. J. Liu  
Pacific Northwest National Laboratory  
Richland, WA 99352, USA  
E-mail: Jun.Liu@pnnl.gov

Dr. Y. Cao  
College of Chemistry and Molecular Science  
Wuhan University,  
Wuhan 430072, P. R. China  
E-mail: ylcao@whu.edu.cn

Dr. L. Xiao  
College of Chemistry  
Central China Normal University  
Wuhan 430079, P. R. China



DOI: 10.1002/adma.201103392

was reported that PAN became dehydrogenated and cyclized at 450 °C, and all sulfur reacted with PAN to form a heterocyclic polymer interconnected with disulfide bonds on the side chain. The chemically bonded sulfur showed good cycling retention of 90% up to 380 cycles,<sup>[10d]</sup> but the capacity (470 mAh g<sup>-1</sup>) and operating voltage (lower than 2.0 V) were relatively low. Regardless, these results show that organic disulfides bonded on the polymer chains have good electrochemical reversibility and the polymer backbone is stable during electrochemical cycling.

In this paper, we report the synthesis of self-assembled polyaniline nanotubes (PANI-NT) for sulfur encapsulation. The synthesis process for this polymer backbone is very simple and environmentally friendly. The polymer is treated at 280 °C with sulfur so a fraction of elemental sulfur reacts with the polymer to form a three-dimensional, cross-linked, structurally-stable sulfur-polyaniline (SPANI-NT) polymer backbone with both inter- and/or intra-chain disulfide bonds interconnected through in situ vulcanization. This SPANI-NT polymer molecular framework provides strong physical and chemical confinement to the elemental sulfur and the resident polysulfide. In addition, the soft polymer matrix and nanostructures developed in this study can allow reversible in situ deposition of intermediate polysulfide species during discharge and their subsequent transformation during recharge within the polymer matrix, and accommodate the voluminal change associated with the electrochemical reactions. As a result, the as-synthesized SPANI-NT/S composite exhibited superior cycling stability and rate capability.

The scanning electron microscopy (SEM) image of PANI-NT in **Figure 1a** shows a uniform, nanotube structure that is ~150 nm in diameter and several micrometers in length (**Figure 1a** and **Figure S1a**). The surface of PANI-NT appears to be very rough, with many hemispheric particles protruding from the surface (inset in **Figure 1a** and **Figure S1b**). From the

end cross-section, the hollow structure of the nanotubes can clearly be seen (**Figure S1b**). The transmission electron microscopy (TEM) image in **Figure 1b** shows that the diameter of the internal hollow tubes is about 20 nm, and the walls of PANI-NT are composed of nanoparticles and the protruding particles are embedded in the walls. After PANI-NT was heat treated with sulfur at a ratio of 1:4 in a sealed vessel filled with inert argon, the tube structure of the polymer backbone was maintained. However, the surface of the nanotubes becomes smoother, and the diameter increases to 300 nm (**Figure 1c**). The hollow interior of the tube structure also is visible (**Figure 1d**). The presence of sulfur can be detected by electron energy dispersive spectroscopy (EDS) and other techniques, but no large sulfur particles were observed on the nanotubes.

**Figure 2a** shows the Fourier transform infrared (FTIR) spectra of the neat PANI-NT and SPANI-NT/S composite obtained in the 900 to 2000 cm<sup>-1</sup> wave-number range. The spectral characteristics of the neat PANI-NT indicate an emeraldine salt structure.<sup>[11]</sup> The spectrum of the SPANI-NT/S composite is significantly different from the neat polymer. The C = C stretching vibration at 1497 cm<sup>-1</sup> assigned to benzenoid rings shifts to lower wave numbers. The shift is probably caused by the substitution of H atoms on benzenoid rings by S atoms. The C-N stretching vibrational bands in the 1400 to 1200 cm<sup>-1</sup> range also shift to lower wave numbers. The intensity of the C-H vibrational band in the vicinity of 1172 cm<sup>-1</sup> significantly weakens, further confirming the replacement of H atoms on aromatic rings by S atoms. Furthermore, two new bands appear in the vicinity of 996 and 928 cm<sup>-1</sup>. It is known that elemental sulfur shows no vibrational activity in the 900 to 2000 cm<sup>-1</sup> range; therefore, the two new peaks should originate from the vibrations of aromatic rings (Ar)-S and Ar-S-S-Ar, respectively.<sup>[10a]</sup> These results confirm that during the heat treatment, sulfur reacts with the unsaturated bonds in the polymer chains to form cross-linked, stereo-network structures. This process is also known as “vulcanization reaction,” a process used to vulcanize rubber.<sup>[12]</sup> The vulcanization reaction could take place between any two neighboring benzene rings of either inter- or intra-molecularly to form disulfide bonds.

**Figure 2b** shows the XRD patterns of elemental sulfur, the neat PANI-NT, and SPANI-NT/S composite. The XRD pattern of elemental sulfur exhibits some sharp and strong peaks throughout the entire diffraction range, indicating a well-defined crystal structure. The neat PANI-NT shows two broad peaks centered at  $2\theta = 20.2$  and  $25.5^\circ$ , which are attributed to the periodicity parallel and perpendicular to the polyaniline chains.<sup>[13]</sup> The broad, low-intensity peaks suggest that PANI-NT exhibits a typical amorphous structure.<sup>[13,14]</sup> For the SPANI-NT/S composite, the diffraction peaks of elemental sulfur are visible although the intensities become distinctly lower and the full widths at half maximum (FWHM) become broader (**Table S1**), indicating good dispersion of sulfur within the polymer structure. However, because of the higher loading of sulfur, some sulfur incorporated in the polymer network nucleated to form sulfur particles. Thermogravimetric analysis (TGA) revealed that the amount of elemental sulfur was 62% (**Figure S2**). Thus, based on the FTIR, XRD and TGA data, we concluded that, during the vulcanization process, a small amount of elemental sulfur reacts with polyaniline to form a

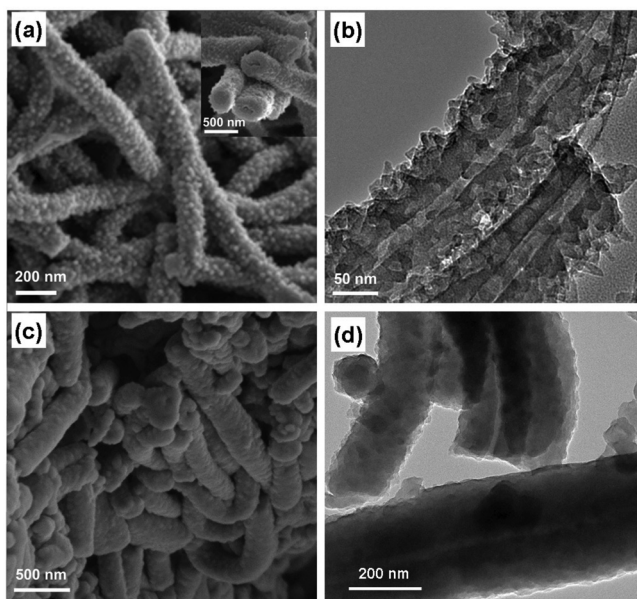


**Figure 1.** SEM (a) and TEM (b) images of the neat PANI-NT. SEM (c) and TEM (d) images of the SPANI-NT/S composite.

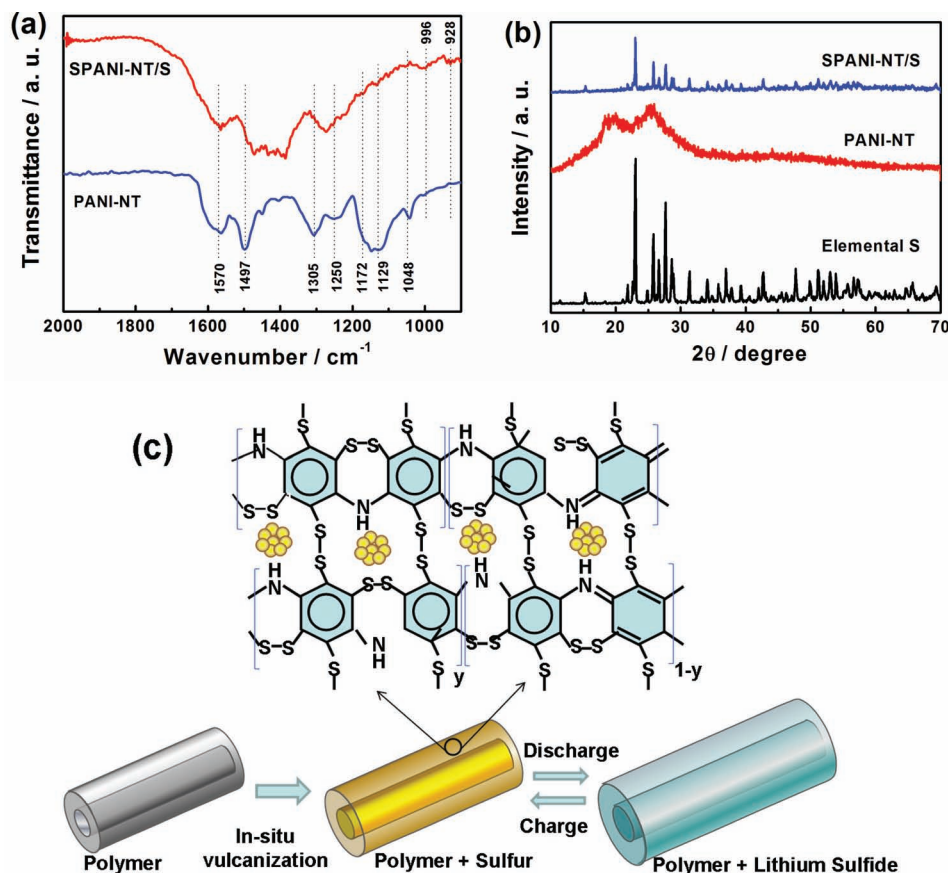


**Figure 2.** (a) FTIR spectra of the neat PANI-NT and SPANI-NT/S composite. (b) X-ray diffraction (XRD) patterns of elemental sulfur, the neat PANI-NT and SPANI-NT/S composite. (c) Schematic illustration of the construction and discharge/charge process of the SPANI-NT/S composite.

cross-linked stereo SPANI network with both inter- and/or intra-chain disulfide bond interconnectivity, and the rest of the melted elemental sulfur concurrently diffuses into the newly formed polymer networks or infuses into the hollow voids. It should be noted that sulfur is both physically and chemically confined in the nanotubes at molecular level. A possible structure for the SPANI-NT/S composite is shown in Figure 2c.

**Figure 3a** shows the cyclic voltammograms of the SPANI-NT/S electrode. The plot shows characteristics typical of the elemental sulfur electrochemical reaction.<sup>[15]</sup> During the cathodic scan, two discrete reduction peaks positioned around 2.3 and 2.0 V were observed, indicating a two-step reduction of elemental sulfur. The first reductive peak at ~2.3 V corresponds to the transformation of cyclo-octasulfur (S<sub>8</sub>) to long-chain soluble lithium polysulfides (Li<sub>2</sub>S<sub>n</sub>, 4 ≤ n < 8). The second peak at ~2.0 V is attributed to the decomposition of the polysulfides to form insoluble short-chain lithium sulfides (Li<sub>2</sub>S<sub>2</sub> and/or Li<sub>2</sub>S). In the subsequent anodic scan, only one intense oxidation peak was found at ~2.6 V because of the slow oxidation kinetics of lithium sulfide to lithium polysulfides. In the following scans up to 10 cycles, the redox peak currents and potentials show no obvious change, which indicates good reactive reversibility and cycling stability of the composite electrode. Besides, the high anodic base line current at 3.0 V is likely caused by some degree of shuttling reaction still presented in the system.<sup>[15b]</sup>

**Figure 3b** shows the initial galvanostatic discharge/charge profiles of the SPANI-NT/S composite electrode at 0.1 C rate (1 C = 1680 mA g<sup>-1</sup>). The SPANI-NT/S composite electrode shows two apparent discharge plateaus and one charge plateau, which agree well with the current peaks in the CV plots (**Figure 3a**). The capacity of elemental sulfur was calculated by deducting the capacity contribution from the SPANI-NT backbone. Therefore, the discharge capacity of the SPANI-NT/S composite during the first discharge was 755 mAh g<sup>-1</sup>. At higher discharge rates of 0.5 and 1 C, the electrode delivered a capacity of 487 and 511 mAh g<sup>-1</sup>, respectively (See **Figure 3c**). Although relatively low initial discharge capacities occurred at different charge/discharge rates, the electrodes showed a gradual increase in discharge capacities during the initial several tens of cycles (**Figure 3c** and **Figure S3**). This behavior indicates that the SPANI-NT/S composite electrode requires an activation step. The possible reason for the activation process is that the surface area of the as-prepared SPANI-NT/S composite is low compared with a carbon/sulfur composite; therefore, it takes some time for the electrolyte to flood the internal surfaces of the polymers. Some of the deeply buried sulfur and disulfide bonds gradually become electrochemically active only when they come into contact with the electrolyte. Subsequently, the capacities at different discharge rates almost stabilized and demonstrated little fading upon extended cycling. The electrode retained capacities

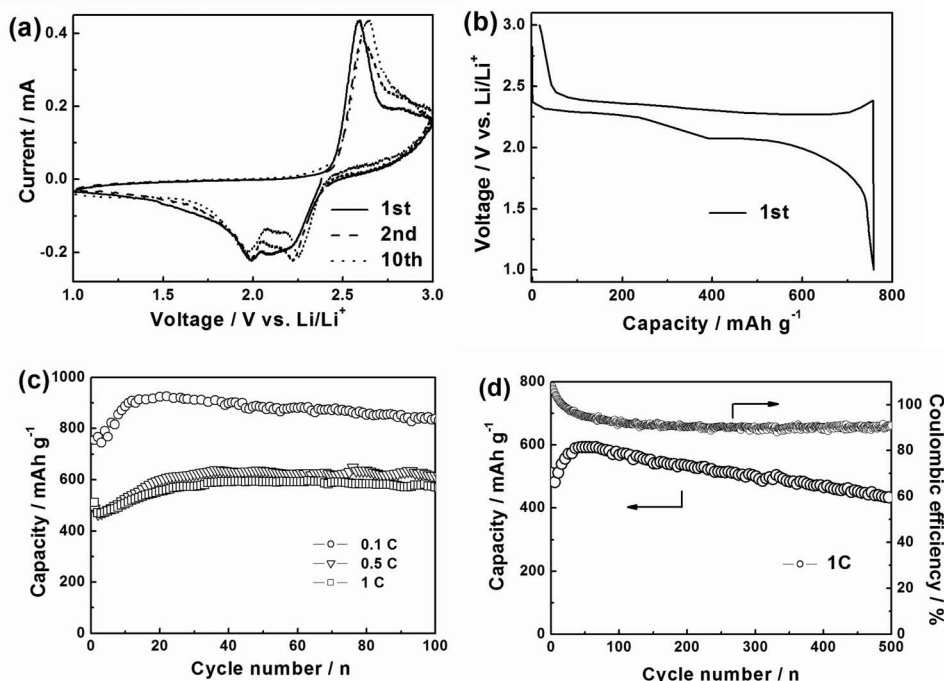


**Figure 3.** (a) Cyclic voltammograms of the SPANI-NT/S composite electrode at  $0.1 \text{ mV s}^{-1}$  at 1.0 to 3.0 V vs.  $\text{Li/Li}^+$ . (b) Initial discharge/charge cycle of the electrode at a 0.1 C rate at 1.0 to 3.0 V vs.  $\text{Li/Li}^+$ . (c) Discharge capacities vs. cycle numbers of the electrode at different rates as labeled. (d) Prolonged cycling performance and coulombic efficiency of the electrode up to 500 cycles at 1 C rate.

of 837, 614, and 568  $\text{mAh g}^{-1}$  after 100 cycles at 0.1, 0.5, and 1 C rates, respectively. Even after very-long-term cycling of 500 cycles, a discharge capacity of 432  $\text{mAh g}^{-1}$  was obtained at 1 C rate, which corresponded to a 76% capacity retention ratio as shown in Figure 3d. Besides, the coulombic efficiency still remained over 90%. We should point out that although this composite showed better cyclability for up to 500 cycles, some capacity degradation is still observed. There might be two reasons: (1) There might still be some dissolution and shuttling of the S species. (2) The in situ formed SPANI polymer framework is electrochemically active, so the disulfide bonds split and recombine during discharge/charge. It is possible that some of the dissociated disulfide bonds cannot recover to the original crosslinked state, causing a decrease in the stability of the polymer matrix.

The excellent rate cycling stability of the SPANI-NT/S composite electrode could be related to the SPANI-NT polymer framework, which provides a three-dimensional, molecular-level capsule to contain the sulfur compounds, as compared to the nanoscale encapsulation by mesoporous carbon. Furthermore, SPANI-NT is a flexible and reactive structural host compared with rigid carbon materials. Due to the lower volume density of  $\text{Li}_2\text{S}$  ( $1.67 \text{ g cm}^{-3}$ ) than S ( $2.03 \text{ g cm}^{-3}$ ), the S electrodes have to bear mechanical stress caused by volume changes in a large measure during cycling. As it was found that the thickness of a carbon/S composite electrode changed by about 22% after one discharge/charge cycle.<sup>[16]</sup> In this case, during discharge, elemental sulfur is converted into polysulfides and  $\text{Li}_2\text{S}$ , meanwhile, some of the disulfide bonds connected to the SPANI-NT/S polymer may split into dithiolates; therefore, the polymer

matrix can expand concurrently with the transition from S to  $\text{Li}_2\text{S}_2$  and/or  $\text{Li}_2\text{S}$ . During successive charge, the volume of  $\text{Li}_2\text{S}$  shrinks when it converts to sulfur, simultaneously, the polymer volume decreases when the disulfide bonds recombine; therefore, mechanical stress arising from the electrochemical reaction is effectively alleviated.

This reversible change in morphology is demonstrated by the fresh, discharged and recharged SPANI-NT/S composite electrodes. The morphology of the fresh electrode were shown in Figure 4a and magnified in Figure 4b. After being fully discharged (Figure 4c), the polymer tubes are deformed into a swollen, sausage-like structure. The surface becomes much smoother than that of fresh samples, probably because of the precipitation of a thin layer of discharge products ( $\text{Li}_2\text{S}_2$  and/or  $\text{Li}_2\text{S}$ ). It is also noticeable that the diameter of the discharged SPANI-NT/S tubes becomes thicker than the refresh ones indicating the flexibility of the interwoven host structure. After recharged to 3.0 V (Figure 4d), not only the dimensions of the nanotubes revert to that of the fresh ones, but also the surface of the recharged nanotubes becomes less smooth again. Obviously, the rough nanotube morphology is restored similar to that of the fresh sample (Figure 4b). These observations strongly suggest that the soft polymer nanotubes can support and accommodate the charge/discharge reactions reversibly.

Figure 4e shows the XPS spectra in the S 2p region. For the fresh electrode, the fitted curves clearly show two energy peaks positioned at 163.9 and 165.1 eV, which are corresponding to the S 2p<sub>3/2</sub> and S 2p<sub>1/2</sub> components respectively. After discharged to 1.0 V, the S 2p peaks shift towards lower binding energy and decompose into two doublets peaks. The doublet located at

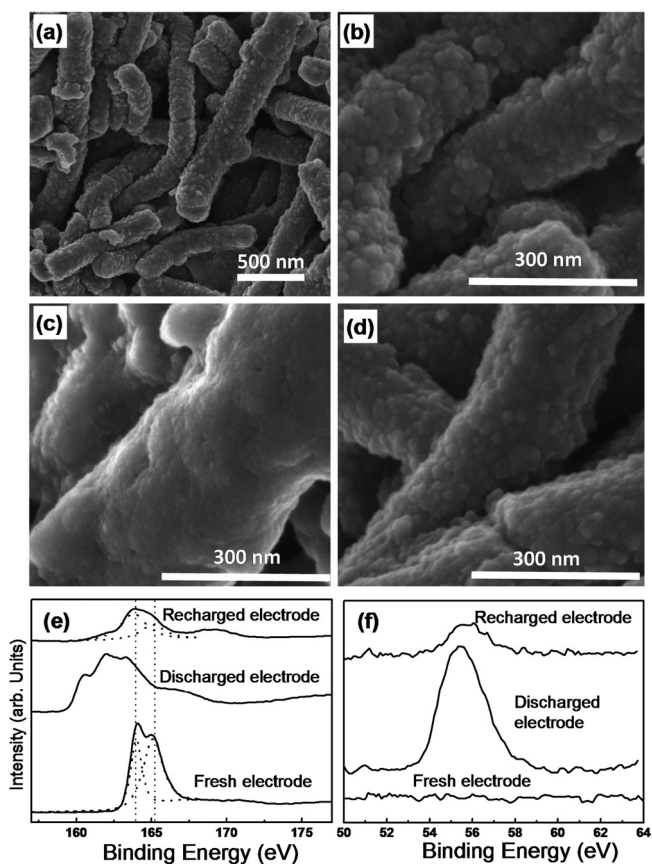


**Figure 4.** SEM images of the SPANI-NT/S composite electrodes: (a) the fresh electrode, (b) high magnification of (a), (c) the electrode first discharged to 1.0 V, and (d) the electrode recharged to 3.0 V restoring the morphology to (a). XPS spectra for the SPANI-NT/S electrode: (e) the S 2p spectra (the fitted curves are shown in dash line) and (f) the Li 1s spectra at different charge/discharge states as labeled.

160–162 eV are assigned with  $S^{2-}$  ion,<sup>[17]</sup> while the doublet positioned at higher binding energy may be associated to  $S_2^{2-}$  ion. When the electrode was recharged, the S 2p peaks move back to binding energy region similar to the fresh electrode, implying that lithium sulfides was recharged back to elemental S and fulfilled a reversible electrochemical process, except that the peaks become broader likely due to a more heterogeneous environment after reaction. Besides, a broad weak peak occurred at higher binding energy range (170 eV on both the fresh and recharged electrodes, which may arise from high valent sulfur ions probably formed by elemental sulfur reacting with trace oxygen during the vulcanization process. At the same time, the Li 1s spectrum signals also display similar reversibility. As shown in Figure 4f, an intensive Li 1s signal peak is observed at the discharged electrode, while it is not observed on the fresh electrode because no lithium exists at this stage. It is important that the Li peak from  $Li_2S/Li_2S_2$  signal becomes very weak on the recharged electrode, implying that most of  $Li_2S$  converts to soluble lithium salt in the electrolyte, which is consistent with the charge/discharge reaction mechanism of sulfur electrode. Overall, the XPS results agreed well with the SEM observations (Figure 4a–d).

In conclusion, a novel SPANI-NT/S molecular composite was synthesized in nanotube form via an in situ vulcanization process by heating a mixture of PANI-NT and sulfur at 280 °C. The electrode could retain a discharge capacity of 837 mAh g<sup>-1</sup> after 100 cycles at a 0.1 C rate. Even at a high discharge rate of 1 C, the electrode manifested very stable cycling capacity up to 500 cycles. Several factors have contributed to the reliable rate cycling observed in the SPANI-HWN/S composite. First, the vulcanization process produces a three-dimensional, cross-linked SPANI network that provides molecular-level encapsulation of the sulfur compounds. Second, the polymer matrix SPANI functions as a self-breathing, flexible framework during charge/discharge to reduce stress and structural degradation. The soft polymer matrix can accommodate the reversible electrochemical reaction and conversion of elemental sulfur and lithium sulfide compounds as well as the voluminal change. In addition, the electropositive amine and imine groups on the SPANI chains further attract polysulfides through electrostatic forces, thereby reducing the displacement of sulfur during repeated cycling. The unique properties of the soft polymer plus their simple fabrication make this class of materials attractive for further investigation for Li-S batteries applications. The properties of the soft polymer nanostructures are different from those of rigid carbon materials, and the combination of the complementary properties may further improve the stability of Li-S batteries.

## Supporting Information

Supporting Information is available from the Wiley Online Library or from the author.

## Acknowledgements

This research is supported by the U.S. Department of Energy (DOE), Office of Basic Energy Sciences, Division of Materials Sciences and Engineering under Award KC020105-FWP12152. The TEM and XPS were conducted at the Environmental and Molecular Sciences Laboratory, a national scientific user facility sponsored by the Department of Energy's Office of Biological and Environmental Research and located at Pacific Northwest National Laboratory. Pacific Northwest National Laboratory (PNNL) is a multiprogram national laboratory operated for DOE by Battelle under Contract DE-AC05-76RL01830.

Received: September 2, 2011  
Revised: December 16, 2011  
Published online: January 25, 2012

- [1] M. Armand, J. M. Tarascon, *Nature* **2008**, 451, 652.
- [2] R. D. Rauh, K. M. Abraham, G. F. Pearson, J. K. Surprenant, S. B. Brummer, *J. Electrochem. Soc.* **1979**, 126, 523.
- [3] S. E. Cheon, K. S. Ko, J. H. Cho, S. W. Kim, E. Y. Chin, H. T. Kim, *J. Electrochem. Soc.* **2003**, 150, A800.
- [4] Y. V. Mikhaylik, J. R. Akridge, *J. Electrochem. Soc.* **2004**, 151, A1969.
- [5] a) L. X. Yuan, J. K. Feng, X. P. Ai, Y. L. Cao, S. L. Chen, H. X. Yang, *Electrochem. Commun.* **2006**, 8, 610; b) J. H. Shin, E. J. Cairns, *J. Power Sources* **2008**, 177, 537.
- [6] a) X. L. Ji, K. T. Lee, L. F. Nazar, *Nat. Mater.* **2009**, 8, 500; b) N. Jayaprakash, J. Shen, S. S. Moganty, A. Corona, L. A. Archer,

- Angew. Chem. Int. Ed.* **2011**, *50*, 5904; c) S.-R. Chen, Y.-P. Zhai, G.-L. Xu, Y.-X. Jiang, D.-Y. Zhao, J.-T. Li, L. Huang, S.-G. Sun, *Electrochim. Acta* **2011**, *56*, 9549; d) B. Zhang, X. Qin, G. R. Li, X. P. Gao, *Energy Environ. Sci.* **2010**, *3*, 1531.
- [7] a) Y. L. Cao, X. L. Li, I. A. Aksay, J. Lemmon, Z. M. Nie, Z. G. Yang, J. Liu, *Phys. Chem. Chem. Phys.* **2011**, *13*, 7660; b) H. Wang, Y. Yang, Y. Liang, J. T. Robinson, Y. Li, A. Jackson, Y. Cui, H. Dai, *Nano Lett.* **2011**, *11*, 2644; c) L. Ji, M. Rao, H. Zheng, L. Zhang, Y. Li, W. Duan, J. Guo, E. J. Cairns, Y. Zhang, *J. Am. Chem. Soc.* **2011**, *133*, 18522.
- [8] X. Ji, S. Evers, R. Black, L. F. Nazar, *Nat. Commun.* **2011**, *2*, 325.
- [9] a) F. Wu, S. X. Wu, R. J. Chen, J. Z. Chen, S. Chen, *Electrochem. Solid State Lett.* **2010**, *13*, A29; b) F. Wu, J. Z. Chen, R. J. Chen, S. X. Wu, L. Li, S. Chen, T. Zhao, *J. Phys. Chem. C* **2011**, *115*, 6057; c) J. Wang, J. Chen, K. Konstantinov, L. Zhao, S. H. Ng, G. X. Wang, Z. P. Guo, H. K. Liu, *Electrochim. Acta* **2006**, *51*, 4634; d) M. M. Sun, S. C. Zhang, T. Jiang, L. Zhang, J. H. Yu, *Electrochem. Commun.* **2008**, *10*, 1819; e) L. L. Qiu, S. C. Zhang, L. Zhang, M. M. Sun, W. K. Wang, *Electrochim. Acta* **2010**, *55*, 4632.
- [10] a) X. G. Yu, J. Y. Xie, J. Yang, H. J. Huang, K. Wang, Z. S. Wen, *J. Electroanal. Chem.* **2004**, *573*, 121; b) J. L. Wang, J. Yang, J. Y. Xie, N. X. Xu, *Adv. Mater.* **2002**, *14*, 963; c) J. L. Wang, J. Yang, C. R. Wan, K. Du, J. Y. Xie, N. X. Xu, *Adv. Funct. Mater.* **2003**, *13*, 487; d) X. U. Yu, J. Y. Xie, Y. Li, H. J. Huang, C. Y. Lai, K. Wang, *J. Power Sources* **2005**, *146*, 335.
- [11] a) A. Kellenberger, E. Dmitrieva, L. Dunsch, *Phys. Chem. Chem. Phys.* **2011**, *13*, 3411–3420; b) M. Trchova, P. Matejka, J. Brodinova, A. Kalendova, J. Prokes, J. Stejskal, *Polym. Degrad. Stabil.* **2006**, *91*, 114–121.
- [12] M. Akiba, A. S. Hashim, *Prog. Polym. Sci.* **1997**, *22*, 475.
- [13] Q. M. Jia, S. Y. Shan, L. H. Jiang, Y. M. Wang, *J. Appl. Polym. Sci.* **2010**, *115*, 26.
- [14] G. Y. Zhao, H. L. Li, *Micropor. Mesopor. Mater.* **2008**, *110*, 590–594.
- [15] a) D. H. Han, B. S. Kim, S. J. Choi, Y. J. Jung, J. Kwak, S. M. Park, *J. Electrochem. Soc.* **2004**, *151*, E283; b) J. Shim, K. A. Striebel, E. J. Cairns, *J. Electrochem. Soc.* **2002**, *149*, A1321.
- [16] S. E. Cheon, S. S. Choi, J. S. Han, Y. S. Choi, B. H. Jung, H. S. Lim, *J. Electrochem. Soc.* **2004**, *151*, A2067.
- [17] a) C. M. Fang, H. C. Gao, Y. Ho, Z. G. Cai, Y. Zhang, *Solid State Ionics* **1991**, *48*, 289; b) J. Li, J. L. Luo, K. T. Chuang, A. R. Sanger, *J. Power Sources* **2006**, *160*, 909.